Laboratory Investigation (2007) 87, 14–28

www.laboratoryinvestigation.org

Lupus resistance is associated with marginal zone abnormalities in an NZM murine model

Biyan Duan[1], Byron P Croker[1,2] and Laurence Morel[1]

[1]*Department of Pathology, Immunology and Laboratory Medicine, University of Florida College of Medicine, Gainesville, FL, USA and* [2]*Pathology and Laboratory Medicine Service, Malcolm Randall Veterans Administration Medical Center, Gainesville, FL, USA*

The NZM2410 and NZM TAN (TAN) are two of 27 inbred strains derived from an intercross between the NZW and NZB strains. NZM2410 mice develop a highly penetrant lupus nephritis mediated by three susceptibility loci, *Sle1*, *Sle2* and *Sle3*. These three loci have been combined on a C57BL/6 background in a triple congenic strain that reconstitutes the NZM2410 autoimmune phenotype. Remarkably, inspite of the presence of *Sle1*, *Sle2* and *Sle3*, TAN mice display a mild autoimmune phenotype reminiscent of NZW. Contrary to the lupus-prone strains, the majority of TAN CD4$^+$ T cells are in a naïve-inactivated stage. TAN mice show B-cell developmental abnormalities similar to lupus-prone mice, such an accumulation of transitional T1 cells and peritoneal B-1a cells. TAN mice show, however, a unique expansion of the splenic marginal zone, in which B cells express high levels of CD5 and CD9, fail to migrate to the follicles in response to LPS, and show sub-optimal binding of T-independent type 2 antigens. Therefore, TAN mice present a functional silencing of marginal zone B cells, which have been previously implicated with autoimmune process. The TAN strain thus provides a novel model for the analysis of the genetic determinants of B-cell autoreactivity.
Laboratory Investigation (2007) **87,** 14–28. doi:10.1038/labinvest.3700497; published online 27 November 2006

Keywords: lupus; mouse; marginal zone; B cells

The New Zealand Mixed (NZM) murine strains are homozygous for variable proportions of the NZB and NZW genomes.[1] Among them, NZM2410 mice develops an accelerated form of systemic autoimmunity and ensuing fatal glomerulonephritis (GN) as compared to the parental (NZB × NZW)F1 (BWF1) mice, a classical systemic erythematosus (SLE) model. Linkage analysis of a cross between NZM2410 and C57BL/6 (B6) and subsequent congenic analysis have identified three lupus susceptible loci, *Sle1* on chromosome 1, *Sle2* on chromosome 4 and *Sle3* on chromosome 7.[2,3] A similar approach conducted in the NZM2328 model has identified susceptibility loci in regions close to *Sle1* and *Sle2*.[4,5] *Sle1*, *Sle2* and *Sle3* represent the three NZM2410 SLE susceptibility loci that are necessary and sufficient for the development of fatal GN on a B6 background in a triple congenic strain, B6.NZM2410.*Sle1.Sle2.Sle3* (B6.TC).[6]

Correspondence: Dr L Morel, PhD, Department of Pathology, Immunology and Laboratory Medicine, University of Florida College of Medicine, PO Box 100275, 1600 SW Archer Road, Gainesville, FL 32610-0275, USA.
E-mail: morel@ufl.edu
Received 10 August 2006; revised 7 October 2006; accepted 8 October 2006; published online 27 November 2006

Potent NZW-derived *Sles* suppressor loci counterbalance these SLE-susceptibility loci,[7] demonstrating that the disease phenotype of a given strain results from the integration of multiple susceptibility and resistance loci.[8]

In the present study, we first present the biologic, histologic and genetic features of an undescribed NZM strain, TAN. The TAN strain carries the same *Sle1*, *Sle2* and *Sle3* susceptibility loci as NZM2410, but displays a dominant resistance to SLE. Although they develop comparable levels of splenomegaly, TAN mice produce significantly less antinuclear antibodies, and do not develop lupus nephritis when followed to 12 months of age. In the second part of this paper, we explore mechanisms that may account for lupus resistance in TAN mice. We show that T-cell activation is profoundly reduced and that peripheral B-cell development is also profoundly altered. Most notably, TAN mice present a great expansion of the B-1a compartment and the splenic marginal zone (MZ), although the percentage of B cells expressing MZ B surface markers was not significantly altered. Both B-1a cells and MZ B cells have been implicated in systemic autoimmunity. These two B-cell compartments, which share many surface markers, are both part of the 'natural immune memory' and are enriched for autoreactive

specificities.[9] B-1a cells are present in increased number and percentage in the BWF1 model,[10] including the NZM2410 and B6.TC strains.[11,12] MZ B-cell numbers are also increased in the BWF1 model,[13] in which they have been implicated in lupus autoimmunity.[14–16] In the TAN mouse, we show that B cells located in the marginal zone express CD5, which is normally present on B-1a cells. CD5, a negative regulator for B-cell receptor (BCR) signaling,[17] may prevent the activation of autoreactive B cells and contribute to the SLE resistance phenotype. In addition, we show that TAN MZ B cells fail to bind T-independent type 2 (TI-2) antigens and to respond to lipopolysaccharide (LPS), two functional characteristics of normal MZ B cells,[18] further indicating that the TAN MZ B compartment has been profoundly altered.

Overall, the TAN mice represent a new model of great value to elucidate the genetic and cellular mechanisms of lupus susceptibility and resistance, and the role played by B-cell peripheral development in the process.

Materials and methods

Mice

Mice were bred and maintained at the Animal Resource Department of the University of Florida in accordance with NIH guidelines and IACUC approval. Initial breeding stocks from B6 and NZM2410 were obtained from the Jackson Laboratories, Bar harbor, ME, and TAN breeding stocks were obtained from Ulrich H Rudofsky, Wadsworth Center for Laboratories and Research, New York State Health Department. The B6.*H-2*^{z} and B6.NZM.*Sle1.Sle2.Sle3* (B6.TC) strains have been described previously.[6,19] Serum was collected bimonthly by tail bleeds for determination of autoantibody levels. A cohort of (B6.TC $\times$ TAN)F_1 hybrids was produced and analyzed in parallel with the parental strains to assess the eventual effects of the TAN genome on the *Sle1*, *Sle2* and *Sle3* loci. These F_1 mice were B6/TAN heterozygous at the entire genome, except NZM2410/TAN heterozygous at *Sle5*, and homozygous at *Sle1*, *Sle2* and *Sle3* (Figure 1). Necropsies were performed when mice were clinically ill or at 12 months of age. Tissues were examined, weighed, snap frozen and/or fixed in 10% buffered formaldehyde.

Genomic Analysis

The NZB or NZW origin of the TAN genome was compared to NZM2410 with 172 microsatellite markers that are polymorphic between the parental strains, as previously described.[7] These markers were distributed across all 19 autosomes with a higher density at the previously characterized *Sle* and *Sles* loci.[2,7] A complete list of these markers and allele segregation between the two strains is available upon request. Segregation of four coat color genes that are polymorphic between NZB and NZW, *Agouti* on chromosome 2, *brown* on chromosome 4, *pink-eye-dilution* and *albino* both on chromosome 7, is identical between TAN and NZM2410.

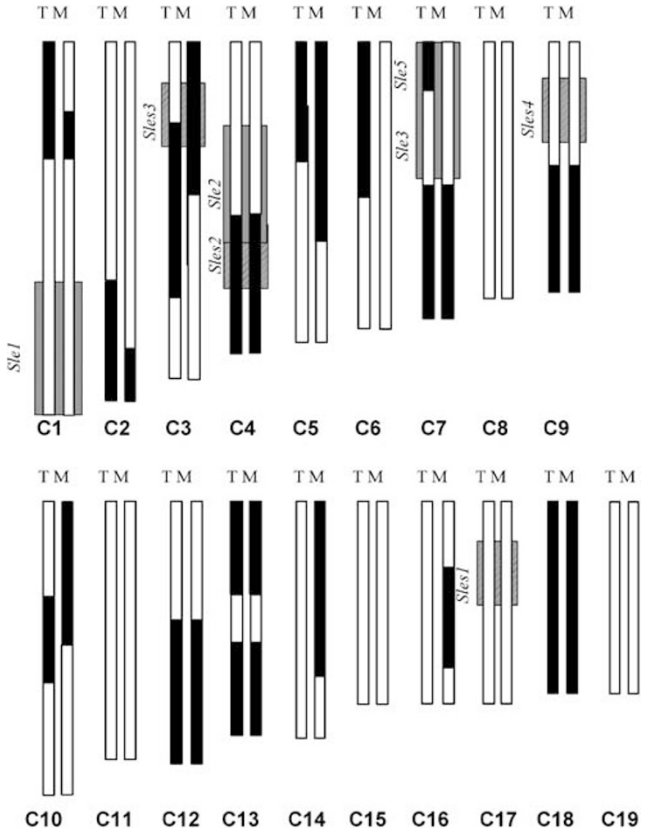

Figure 1 Comparison of the TAN and NZM2410 genomes with microsatellite markers polymorphic between NZB and NZW. Each of the autosomes is represented with the centromere at the top, with black boxes indicating regions from NZB origin and white boxes indicating regions of NZW origin. The TAN chromosomes are on the left (T), and the NZM chromosomes are on the right (M). The three gray boxes show the location of the NZM *Sle* susceptibility loci present in B6.TC. The four hatched boxes show the positions of the NZW-derived *Sles* suppressor loci.

Serologic Studies

IgG autoantibodies directed against dsDNA and chromatin, total IgM and IgG levels were detected by ELISA assays as previously described.[6] Samples with values greater than 2 s.d. from the B6 control mean were considered positive for autoantibodies.

Histology

Major organs were evaluated on hematoxylin and eosin (H&E) and periodic acid Schiff- (PAS) stained sections as previously described.[6] GN was classified and graded based on the modified WHO classification of clinical lupus nephritis[20] combined with

semiquantitative scale.[21] Briefly, glomerular lesions were classified as none, mesangiopathic, proliferative, membranous, crescentic and hyaline as determined by the predominant lesion and based in part on previous studies by us and others. The extent of involvement was based on percentage of glomeruli with lesions and was graded on a 0–4 scale as follows: 0 (none), 1 (1–10%), 2 (11–25%), 3 (26–50%), 4 (>50%). For further clarification, a comparison of this classification with WHO classification shows that a 1, 2 or 3 grade proliferative (P) or hyaline (H) lesion corresponds to focal proliferative GN (WHO Class III) and a grade 4P or H lesion corresponds to diffuse proliferative lupus nephritis (WHO Class IV). For immunofluorescence staining, fresh tissues embedded in OCT were snap-frozen and cut into sections of 6–7 μm in thickness. Acetone-fixed sections were first blocked with 10% rat serum in PBS, then stained with fluorochrome-conjugated monoclonal antibodies (anti-mouse MOMA1-FITC from Serotec (UK), SIGN-R1 (ER-TR9)-biotin from BMA (Switzerland), B220 (RA3-6B2)-APC, IgM (Igh6)-APC, CD1d (1B1)-biotin and hamster IgG1 anti-TNP (A19-3)-biotin were purchased from BD Pharmingen (San Diego, CA). Biotinylated antibodies were further detected with streptavidin-Alexia 568 from Molecular Probes (Carlsbad, CA). Sections were finally washed, mounted with Prolong Gold media from Molecular Probes and analyzed with a Zeiss Axiom fluorescent microscope.

Flow Cytometry

Single cell suspensions from spleen or peritoneal lavage were treated with anti-CD16/32 (clone 2.4G2) in flow cytometry buffer (5% FCS in PBS) for 20 min on ice. For the *in vitro* TNP-Ficoll-binding assay, splenocytes suspensions were incubated with TNP-Ficoll (Biosearch, Novato, CA) at different concentrations for 30 min at 37°C. Samples were then stained for 20 min with fluorochrome- or biotin-conjugated monoclonal antibodies against mouse B220 (RA3-6B2), CD1d (1B1), CD3e (145-2C11), CD4 (H129.19), CD5 (53-7.3), CD9 (KMC8), CD19 (1D3), CD23 (B3B4), CD25 (7D4), CD62L (MEL-14), CD69 (H1.2F3), CD86 (GL1), CD93 (AA4.1), IgM (II/41) and anti-TNP (G235-2356) (all from BD Pharmingen). CD21 was purified from the 7E9 clone (kindly provided by Dr Boackle, University of Colorado, Denver, CO), which binds equally to the CD21 (CR2) NZW and B6 allotypes.[22] Anti-MD-1/RP105 (MD14) antibody was obtained from Ebioscience). Biotinylated antibodies were further detected with Strepavidin PerCP-Cy5.5. Samples were finally analyzed with BD FACSCalibur flow cytometer, and at least 60 000 cells were acquired per sample.

Bone Marrow Chimeras

Bone marrow (BM) chimeras were performed as previously described.[23] T-cell depleted BM from 3 weeks old TAN male mice were transferred intravenously into lethally irradiated MHC-matched B6.*H-2*^{z} At 11 months post-transfer, MZB phenotypes were analyzed by flow cytometry and histology as described above for intact mice and compared to 11-month-old B6, B6.*H-2*^{z} and TAN. B-cell development is indistinguishable between B6 and B6.*H-2*^{z} mice (Morel L, unpublished data).

Treatment of Mice with TI Antigens

Mice (7- to 9-month old, three for each strain) were injected intraperitoneally with 100 μg LPS (Sigma, St Louis, MO) or 30 μg TNP-Ficoll (Biosearch Technol, Novado, CA) in 200 μl sterile saline buffer. Mice were sacrificed 3 h after the LPS treatment and 30 min after the TNP-Ficoll treatment, and spleens were snap-frozen, fixed and stored at −80°C for immunofluorescence staining.

Statistical Analysis

All data were analyzed using the GraphPad Prism 4 software. Depending on whether the data was normally distributed, parametric or nonparametric were used as indicated. When multiple groups were compared, ANOVA was used and selected pair comparisons were computed using the appropriate correction for multiple comparisons. Distributions between two groups were compared using χ^2 tests. Statistical significance was obtained when $P \leq 0.05$.

Results

Genomic Comparison between TAN and NZM2410

Genotyping with 172 polymorphic markers determined that the TAN and NZM2410 genomes were 70 and 73% NZW-derived, respectively (difference not statistically significant). This is consistent with the presumed (NZB × NZW)F_1 × NZW origin of the NZM strains. The two strains share the same allele at about 80% of the markers (137/172), further indicating a high level of genetic similarity. As shown in Figure 1, TAN shares with NZM2410 and consequently B6.TC, the three major SLE susceptibility loci, *Sle1*, *Sle2* and *Sle3*, but not the *Sle5* locus on centromeric chromosome 7.[24] TAN and NZM2410 also share three NZW-derived SLE suppressor loci: *Sles1*, which is linked to H-2^z on chromosome 17, and *Sles4* on chromosome 9.[7] *Sles2*, which overlaps with *Sle2* on chromosome 4, has the NZB-nonsuppressive allele in both TAN and NZM2410, while *Sles3* on chromosome 3 is the only suppressor locus that differs between the two strains, with the NZW suppressive allele in TAN and NZB-susceptibility allele in NZM2410.

Autoimmune Phenotypes

SLE-related phenotypes (mortality, the presence of serum autoantibodies, and the anatomic characterization of lupus nephritis) of TAN and (B6.TC × TAN)F_1 hybrid (F_1) mice were compared with NZM2410, B6.TC and B6 mice. Cumulative mortality at 12 months was high in both NZM and B6.TC mice (90 and 100%, respectively) due to severe lupus nephritis (Figure 2a) as previously described.[1,2,6] In contrast, mortality at this age was lower in the TAN strain (13%) and nil in the F_1, indicating that the survival phenotype of the TAN strain was dominant or that mortality in each of the two strains was due to different recessive mechanisms. All the autoimmune strains had spleen weights four to sixfold greater than those of control B6. Spleen weights of F_1 mice exhibited a modest but significant 25% reduction compared to either parental strain, further supporting the lack of complementation of the two genomes. The penetrance of severe proliferative GN in the strains (defined as grade P3-4) is shown in Figure 2c. Contrary to B6.TC and NZM2410, TAN mice did not develop severe proliferative GN, although 52% exhibited mild GN, primarily mesangiopathic or hyaline forms. This type of mild GN is the renal phenotype seen in NZW mice.[25,26] The F_1 mice presented an intermediate phenotype with 54% of the mice having mild GN and another 29% exhibiting severe GN. Examples of normal (B6), hyaline (TAN), proliferative (B6.TC) and intermediate GN are illustrated in Figure 3. Although the renal lesions were mild in the TAN mice, a statistically significant gender dichotomy similar to what has been described for the BWF1 and NZM models in general was observed, with an overall penetrance of 13% in males and 59% in females (relative risk 2.10 for females, Fisher exact $P = 0.004$).

TAN mice produced anti-dsDNA IgG antibodies at a level that was intermediate between B6 and B6.TC. TAN values were significantly lower than that of B6.TC at 5, 9 and 12 months of age (Figure 4a). Furthermore, the proportion of TAN mice positive for anti-dsDNA antibodies was significantly lower than that of B6.TC at 5 and 9 months of age ($P < 0.05$ and < 0.01, respectively). The anti-dsDNA IgG production by the F_1 mice was similar to TAN at 5 months but increased at 7 months to levels comparable to those of B6.TC (Figure 4a), suggesting that heterozygosity at certain loci delayed autoantibodies production. The antichromatin IgG titers (Figure 4b) and penetrance (data not shown) in TAN and the F_1 comparatively to B6.TC mice were similar to anti-dsDNA. Total serum IgM was significantly elevated in both TAN and B6.TC (Figure 4c), but IgG was elevated only in B6.TC mice (Figure 4d). This suggests that B cell function is abnormal in both TAN and B6.TC mice, but helper T-cell abnormalities further aggravate the B6.TC phenotypes.

TAN Lupus Resistance is Associated with a Decreased T Cell Activation and an Increased B-1a Cell Population

Flow cytometric analyses revealed lymphocyte differences in TAN mice as compared to either lupus-prone NZM2410 and B6.TC mice or B6 controls. The results will be presented as percentages of lymphocytes, although absolutes number showed magnified differences going in the same direction as did percentages (data not shown), due to the differences in total cell numbers secondary to splenomegaly in all three TAN, B6.TC and NZM2410 strains. Both TAN and the lupus-prone strains showed significantly increased T cell (Figure 5a) and decreased conventional $CD5^-$ $B220^{hi}$ B-2 cell (Figure 5b) populations in the spleen. Interestingly, in spite of their increased number, TAN $CD4^+$ T cells were significantly less activated than either B6.TC or NZM2410, and equivalent to B6 levels (Figure 5c and d). Accordingly, the majority of TAN $CD4^+$ T cells expressed a naïve $CD62L^+$ $CD44^-$ phenotype, and the ratio naïve $CD62L^+$ $CD44^-$/effector ($CD62L^+$ $CD44^+$) or memory ($CD62L^-$ $CD44^+$) was significantly higher in TAN mice (mean ± s.e. = 3.26 ± 0.88) than in B6.TC (0.28 ± 0.16, $P < 0.01$), and restored to a level equivalent to B6 (2.18 ± 0.26). We have already

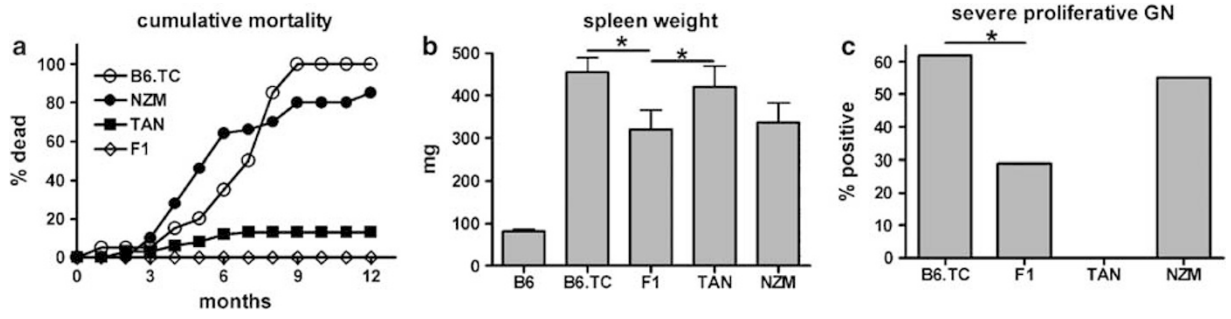

Figure 2 Cumulative mortality (**a**), spleen weight (mean + s.e.) (**b**), and frequency of severe proliferative GN (**c**) in mice aged up to 12 months old with an approximately equal number of males and females for each strain. The number of mice monitored for each strain was: B6: 30, B6.TC: 30, TAN: 60, and (B6.TC × TAN)F_1: 17. NZM2410: 45. For clarity, mortality for B6 mice, which was nil, was not reported in panel a. *$P < 0.05$ of one way ANOVA with Bonferroni post-test correction (**b**) or χ^2 test (**c**).

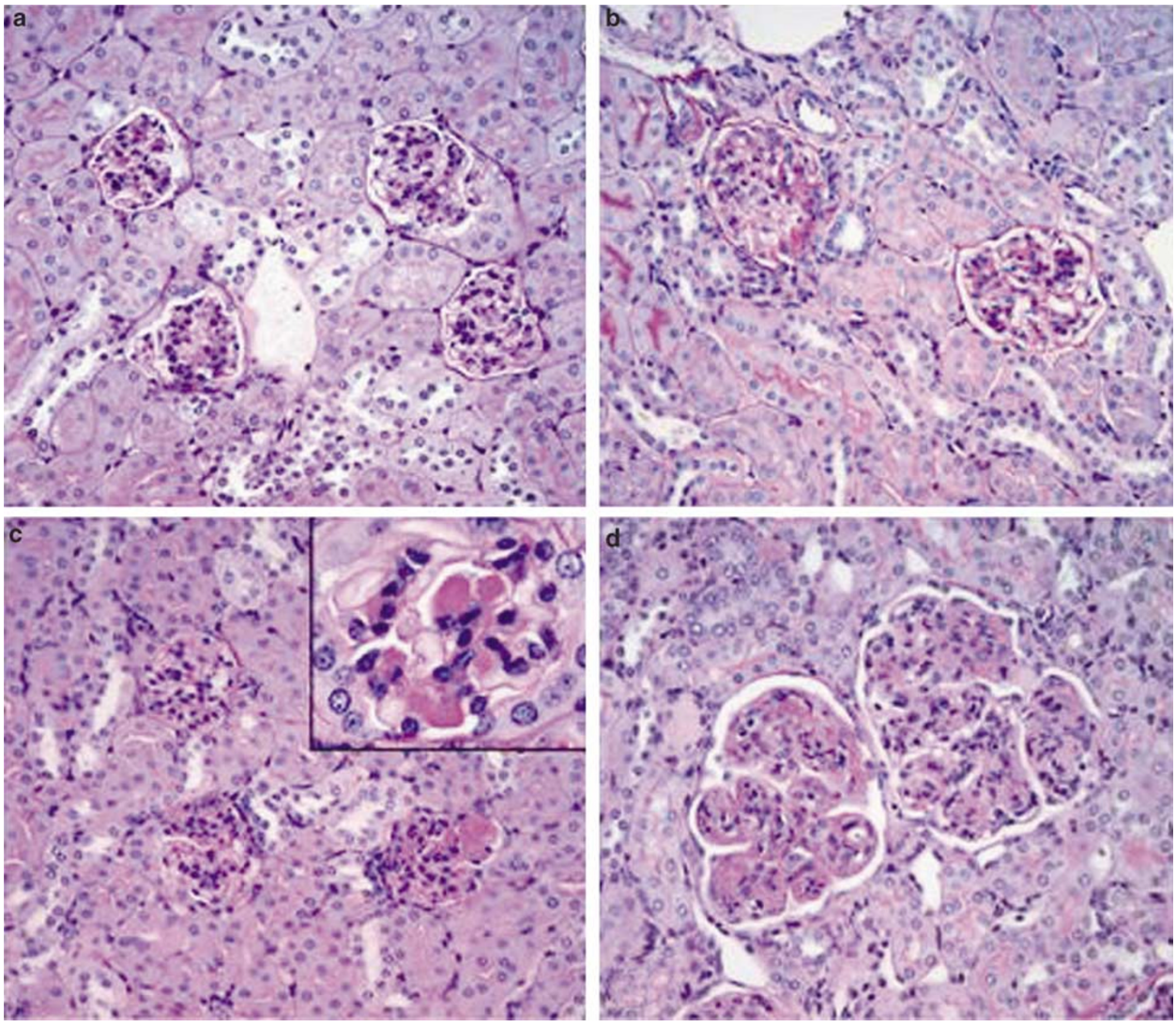

Figure 3 Renal cortex of four strains showing normal (N), mesangopathic (M), hyaline (H) and proliferative (P) histology (PAS, $\times 200$). (**a**) B6 mouse showing four glomeruli with normal morphology (N). (**b**) TAN mouse showing segmental mesangopathic changes in two glomeruli (M). (**c**) (B6.TC $\times$ TAN)F_1 hybrid showing three glomeruli with variable sub-endothelial hyaline deposits increasing in size counter clockwise from upper left glomerulus (none) to lower right glomerulus (most). Inset in upper right is a higher magnification view ($\times 500$) of another glomerulus showing deposits filling or partially filling the sub-endothelial space of several glomerular capillaries (H). (**d**) B6.TC mouse with two enlarged glomeruli showing partial obliteration of capillaries with inflammation and some hyaline deposits (P).

shown that *Sle1* mediates a reduction in the number of $CD4^+$ $CD25^+$ $CD62L^+$ regulatory T cells (Treg).[27] Accordingly, TAN, B6.TC and NZM2410 mice, which all carry *Sle1*, showed a significantly decreased proportion of splenic Treg (Figure 5e), indicating that lupus resistance in TAN mice is not due to a restoration of normal Treg homeostasis. Finally, TAN T cells expressed significantly higher levels of CD5 than B6 (Figure 5f), suggesting that as for the B cells, increased CD5 expression may be a mechanism by which TAN controls T-cell activation.

Only the lupus-resistant TAN mice accumulated splenic $CD5^+$ B-1a cells that were significantly higher than any of the other strains (Figure 5c). On average, the average percentage of TAN splenic B-1a cells was eight times higher than in B6 and almost three times higher than in NZM2410. A different result was obtained in the peritoneal cavity (perC), in which TAN, NZM2410 and B6.TC mice all showed an average three- to eightfolds increase in total cell numbers (data not shown), the majority of which were $CD5^+$ B-1a cells in both NZM2410 and TAN (Figure 5d). The percentage of B-1a cells in B6.TC perC was intermediate between TAN or NZM2410 and B6. These results indicate that the large expansion of TAN splenic B-1a population is not the mere consequence of a general expansion of this B cell compartment, as seen is NZM2410 and B6.TC to a lesser extent, but represents an additional event in which B-1a cells expand in the TAN spleen to the expense of conventional B2 cells.

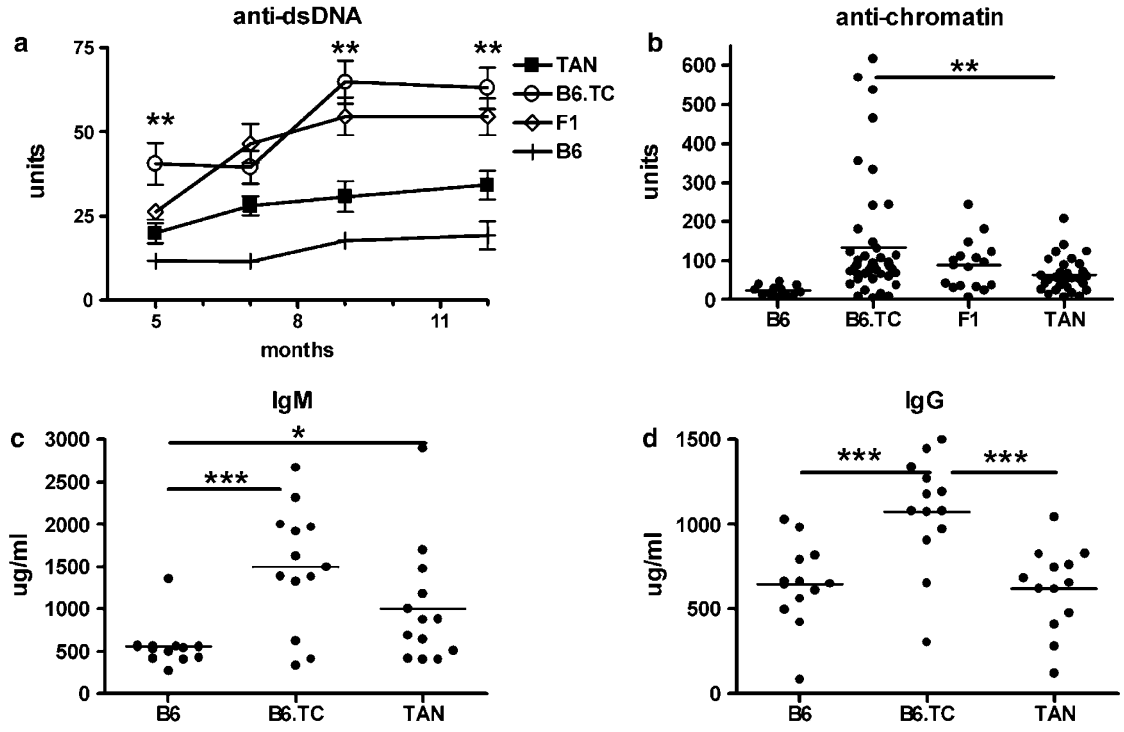

Figure 4 Reduced autoantibody and IgG immunoglobulin production in TAN mice. (**a**) Time course analysis of anti-dsDNA IgG production. Means and s.e. are shown. $^{**}P<0.01$ of one way ANOVA with Bonferroni post-test corrections between B6.TC and TAN values. The F_1 group was significantly lower than B6.TC at 5 months old, but then increased and stayed to similar levels by 7 months old. TAN, B6.TC and F_1 anti-dsDNA IgG levels were significantly higher than B6 at all ages. The number of samples screened in each strain at each time point was between 17 and 30. (**b**) Antichromatin IgG levels at 9 months of age. Although TAN levels were elevated as compared to B6 ($P<0.05$), they were significantly lower than B6.TC ($P<0.01$). Antichromatin levels in the F_1 mice were intermediate between that of TAN and B6.TC. Serum IgM (**c**) and IgG (**d**) in 7 months old mice. IgM was elevated in both TAN and B6.TC, but IgG was only elevated in B6.TC ($^{*}P<0.05$, $^{***}P<0.001$).

TAN Lupus Resistance is Associated with Marginal Zone B Cells Abnormalities

The distribution of the conventional B-cell subsets in the spleen was altered in TAN mice. As we have described previously for NZM2410 and B6.TC,[12] the proportion of transitional T1 B cells was expanded and the proportion of follicular (Fo) B cells was reduced in TAN mice, corresponding to significantly increased T1/Fo ratio (Figure 6a). This was true either when T1 cells were gated as IgM^+ $CD21^{lo/int}$ $CD23^{lo}$ and Fo cells as IgM^+ $CD21^{lo/int}$ $CD23^+$ as shown in Figure 6a, or when T1 cells were gated as $CD93^+$ $B220^+$ IgM^{hi} $CD23^-$ and Fo cells as $CD93^-$ $B220^+$ IgM^{int} $CD23^+$ (data not shown). The percentage of marginal zone (MZ) IgM^{hi} $CD21^{hi}$ $CD23^-$ B cells was more variable in the lupus-prone and resistant mice as compared to B6 (Figure 6b, g and h), but not significantly different when corrections for multiple comparisons were factored in. This was in sharp contrast with the size of the marginal zone has shown by histological examination (Figure 7). Significantly reduced or absent splenic marginal zone areas were observed in both NZM and B6.TC mice. Further histological characterization showed that the MZ B cells that were readily detected by flow cytometry (Figure 6b) are in fact located inside the follicles in the two lupus-prone strains (Duan *et al*, in preparation). In contrast, the lupus-resistant strain TAN showed a markedly enlarged marginal zones. This enlargement was age-dependent, with a normal MZ area in young 2-month-old mice, and a significant expansion in 5- to 6-month-old mice (data not shown). The discrepancy between histological and flow cytometry results prompted us to further examined the surface marker phenotype of TAN MZ B cells. Histological examination indicated that many TAN MZ B cells were $CD5^+$ (Figure 7c). Flow cytometry on MZ B cells gated either as IgM^{hi} $CD1d^{hi}$ or IgM^+ $CD23^-$ $CD21^{hi}$ confirmed that these cells expressed a significantly higher level of CD5 in TAN mice than in any of the other strains examined (Figure 6c and f). These TAN MZ B cells also expressed higher levels of CD9 (Figure 6d), a marker shared by MZ B B-1a cells and plasma cells, and upregulated in MZB cells by LPS exposure.[28] No difference was found, however, for the expression level of IgM, activation markers C80 and CD86, and CXCR5, a chemokine receptor which has been implicated in the migration of the MZ B cells outside the MZ area[29] (data not shown). Furthermore, the number of SIGN-$R1^+$ MZ macrophages, for which a mutual dependence with the number of MZ B cells has been shown,[30,31] was

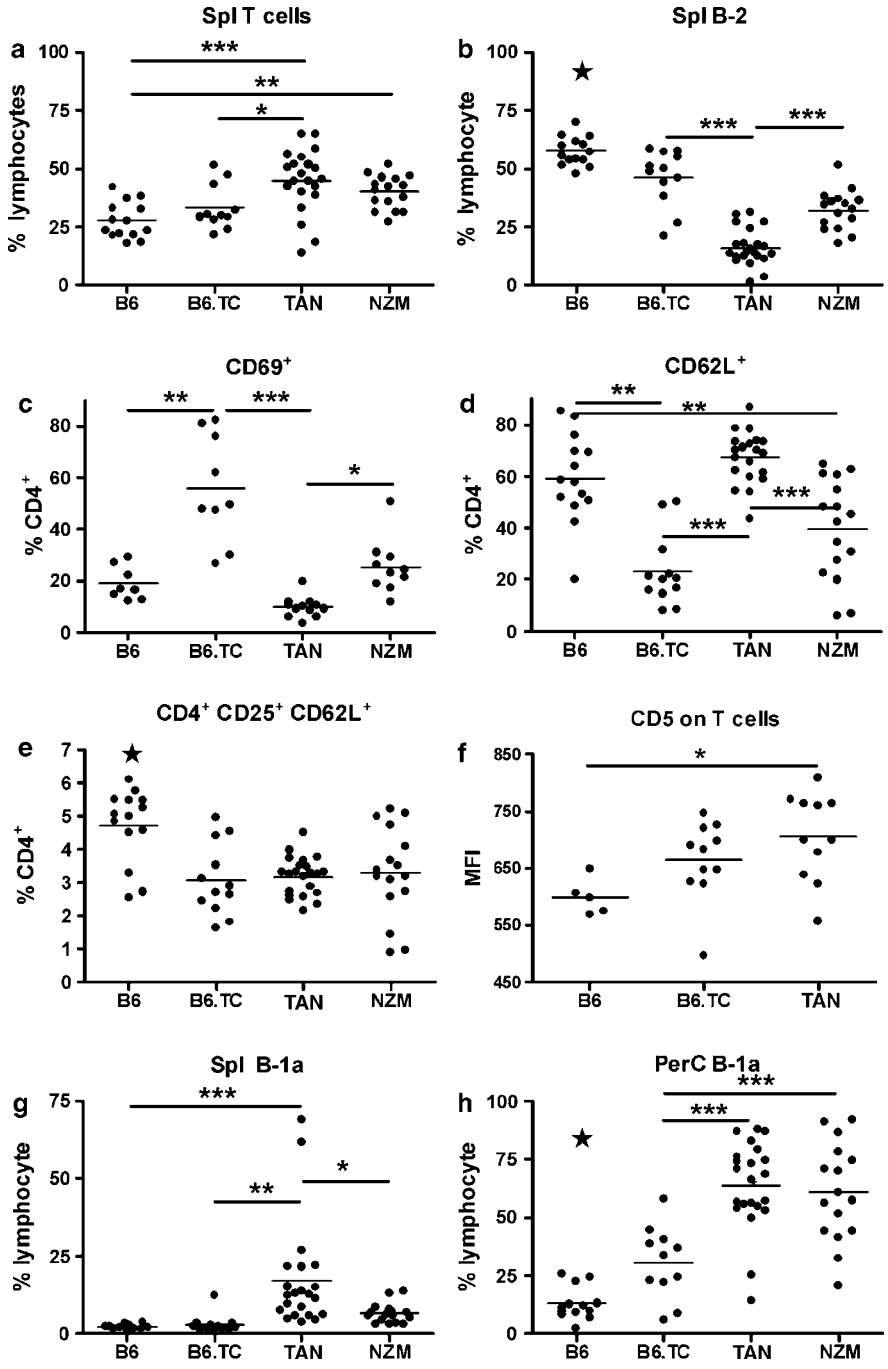

Figure 5 Lymphocyte population distribution and activation in the spleen (**a**–**g**) and peritoneal cavity (**h**) in 8–10 months old mice. (**a**) $CD5^{hi}$ $B220^{-}$ T cells. (**b**) $CD5^{-}$ $B220^{hi}$ B-2 cells. (**c**) Early activation marker CD69 expression on $CD4^{+}$ T cells. (**d**) L selectin CD62L expression on $CD4^{+}$ T cells. (**e**) $CD4^{+}$ $CD25^{+}$ $CD62L^{+}$ Treg. (**f**) CD5 expression on $CD3^{+}$ T cells. $CD5^{+}$ $B220^{lo}$ B-1a cells in the spleen (**g**) and peritoneal cavity (**h**). For each panel, an ANOVA analysis showed highly significant different distribution of values. The pair-wise comparisons indicated on the graphs were performed with Bonferoni's correction. ($^{*}P<0.05$, $^{**}P<0.01$, $^{***}P<0.001$). On panels b, e and h, a star (★) indicates that B6 values were significantly different from all other groups. Otherwise, all significant differences are indicated.

similar between TAN and B6 mice (data not shown). Finally, differences in the recently described MZ B-cell precursor (IgM^{+} $CD93^{-}$ $CD21^{hi}$ $CD23^{+}$) subset[32] could be at the origin of the MZ differences that we observed between lupus-resistant, lupus-prone and controls mice. In old mice, the percentage of splenic MZ B precursors was lower in both TAN and B6.TC than in B6 mice, although statistical significance was achieved only for TAN (data not shown). In 2- to 3-month-old mice in which the marginal zone looks histologically normal for all three strains, a significant reduction of MZ B precursors was observed for both TAN and B6.TC, and the reduction was most pronounced in B6.TC than in TAN (Figure 6e).

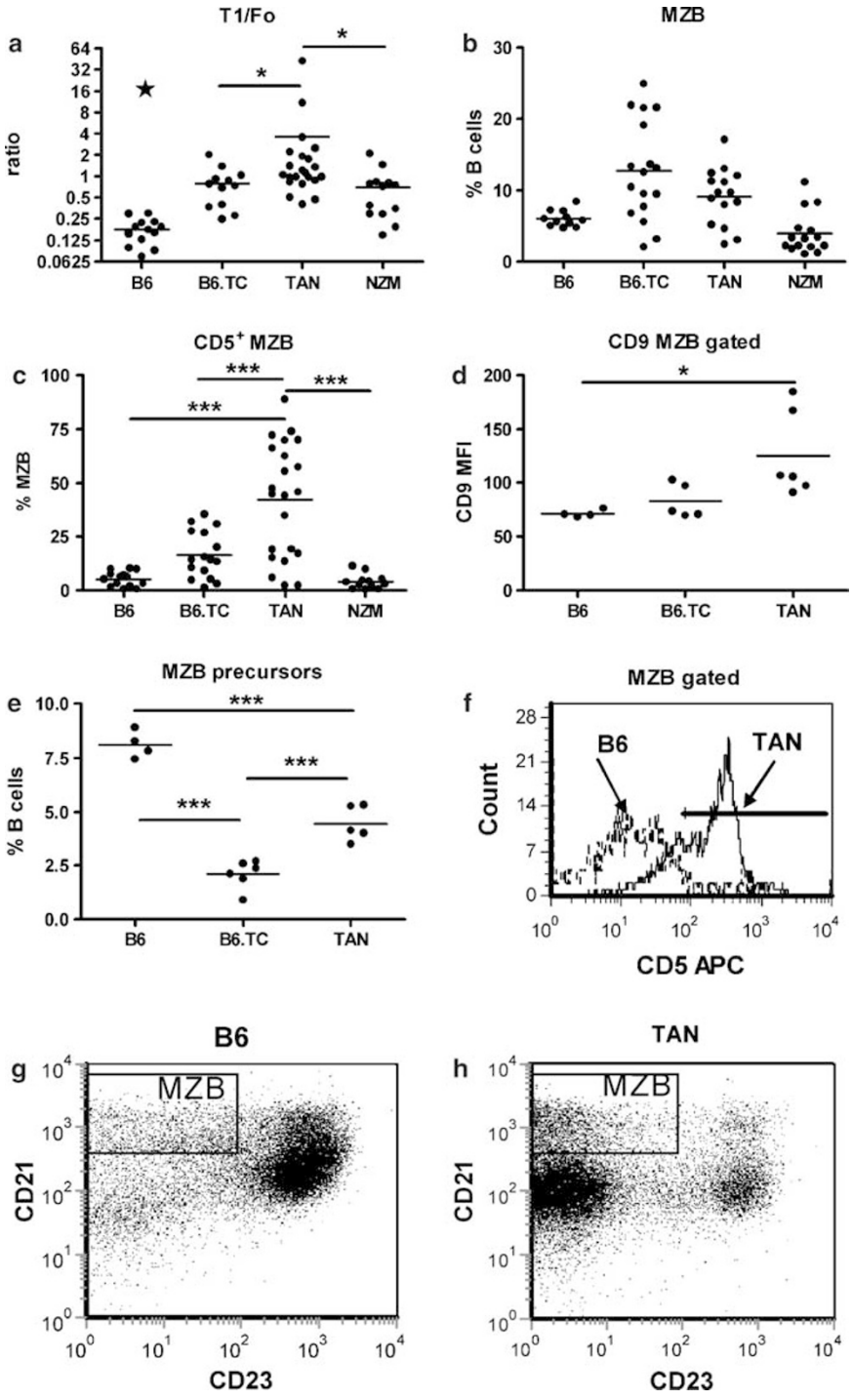

Figure 6 TAN B cells show an abnormal splenic development. (**a**) Transitional T1 over follicular Fo ratio. (**b**) IgM^+ $CD23^-$ $CD21^{hi}$ marginal zone (MZ) B cells expressed as a percentage of IgM^+ splenocytes. (**c**) A significantly higher percentage of MZ B cells express CD5 in TAN than in any of the other strains. (**d**) CD9 expression level was significantly higher on IgM^+ $CD1d^{hi}$ MZ B cells in TAN than in B6 mice. (**e**) Percentage of IgM^+ $CD93^-$ $CD21^{hi}$ $CD23^+$ MZ B precursor cells in 2- to 3-month-old mice. (**f**) Representative CD5 expression on MZ B cells from B6 or TAN mice, according to the gates shown in panels g and h. The position of the marker for positive CD5 staining was determined with an isotype control. (**g**, **h**) Representative IgM^+ gated splenic B6 and TAN cells, showing the $CD21^{hi}$ $CD23^-$ gate for MZ B cells. All mice, except those in panel E were 8–10 months old. For each panel, an ANOVA analysis showed highly significant different distribution of values. The pair-wise comparisons indicated on the graphs were performed with Bonferoni's corrections ($^*P<0.05$, $^{***}P<0.001$). On panel a, a star (★) indicates that B6 was significantly different from all other groups. Otherwise, all significant differences are indicated.

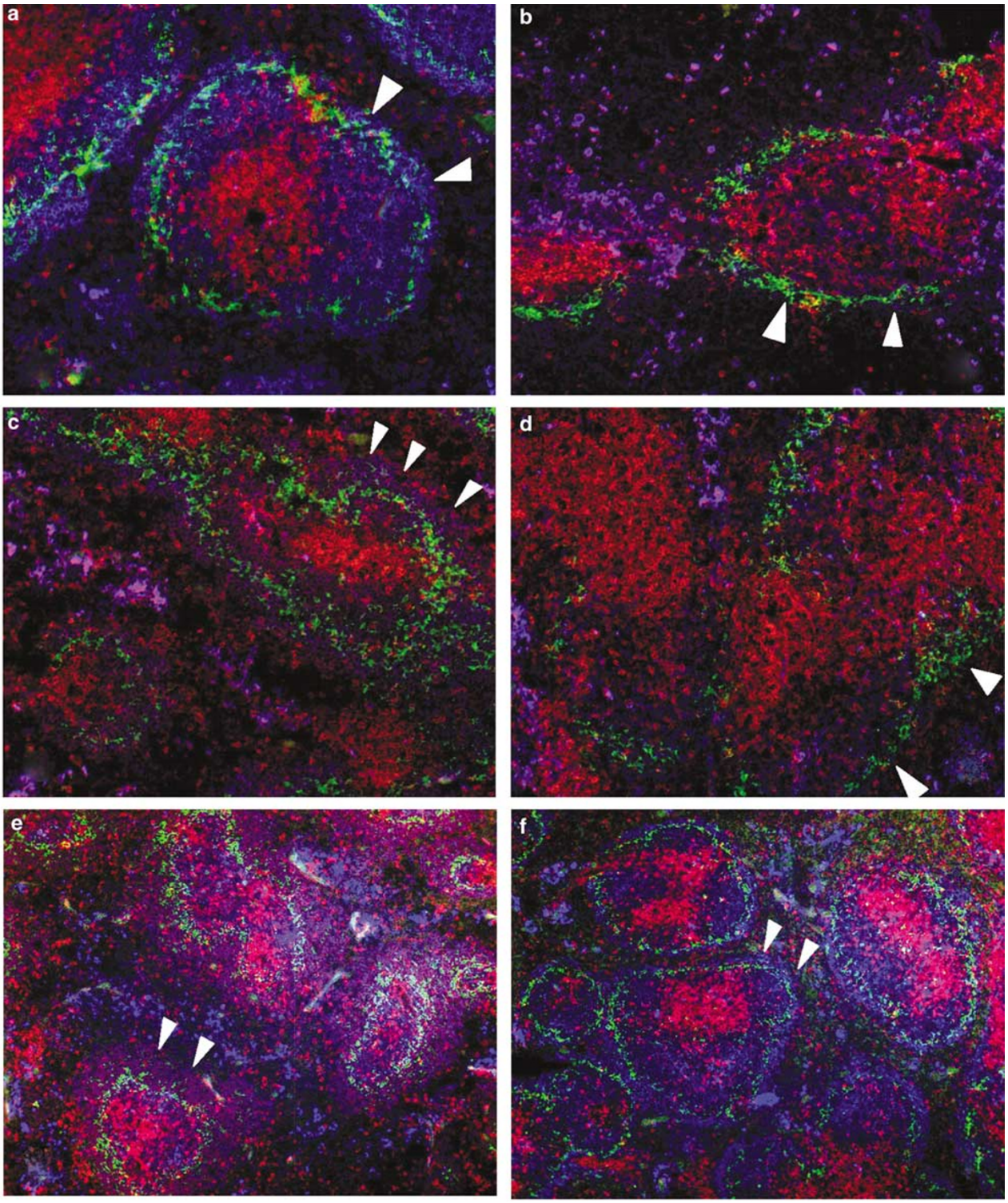

Figure 7 MZ expansion in TAN mice contrasting with MZ reduction in B6.TC and NZM2410. Representative spleen sections slides from 7- to 9-month-old mice (five per strain) stained with FITC conjugated Moma-1 (green), CD5-PE (red) and IgM-APC (blue). Moma-1$^+$ metallophillic macrophages mark the external boundary of the follicle and internal boundary of the marginal zone indicated by arrows. (**a**) B6, representing a normal marginal zone. IgM^{hi} CD5$^-$ MZ B cells are located outside the green ring of Moma-1$^+$ cells. The CD5^{hi} T-cell zone and IgM$^+$ follicular B-cell zone are well defined. (**b**) B6.TC with reduced to absent marginal zone, reduced numbers of follicular B cells, and poorly defined T-cell and B-cell zones. (**c**) TAN, with enlarged MZ area, and many MZ cells expressing both IgM and CD5 (purple). (**d**) NZM2410, which is similar to B6.TC. (**e**) TAN→B6.*H-2*^{z} chimera with enlarged IgM$^+$ CD5$^+$ MZ area. (**f**) B6.*H-2*^{z}, which shows a similar splenic follicular structure as B6. Magnification: ×100.

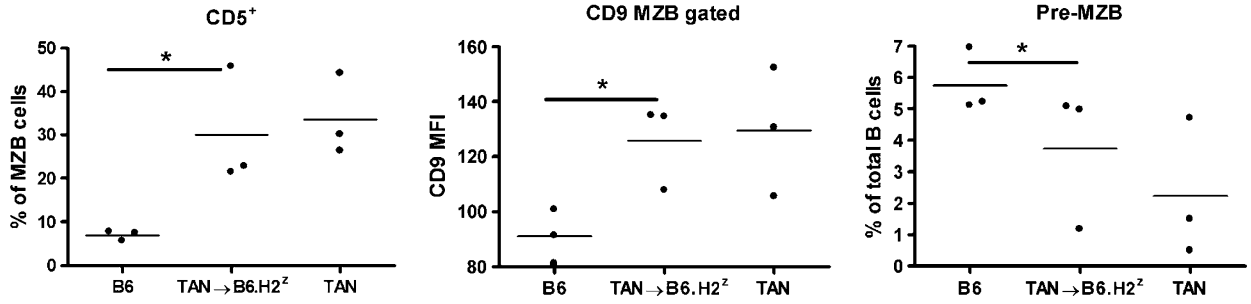

Figure 8 Surface marker phenotypes of MZ B cells in TAN→B6.*H-2*^{z} BM chimeras as compared to aged matched B6 and TAN mice. From left to right, percentage of MZ B cells expressing CD5, CD9 mean fluorescence intensity on MZ B-gated cells and percentage of splenic B cells expressing a precursor MZ B phenotype. *$P<0.05$: Mann–Whitney test between B6 and TAN→B6.*H-2*^{z}.

Consequently, both lupus-prone and lupus-resistant mice show an abnormal development of the MZ B precursor subset, which may be related to the retention of a large number of cells at the T1 stage (Figure 6a). The consequences of this reduced MZ B precursor pool are however, different on the phenotypes of the MZ B cells in each strain.

BM chimeras with TAN BM transferred into lethally irradiated B6.*H2*^{z} hosts showed that the TAN MZ B phenotypes described above are an intrinsic property of TAN hematopoietic cells. CD5 and high CD9 expression, as well as a reduction of the MZ B precursor population were similar between the chimeric and TAN mice, and significantly different from that of B6 (Figure 8). Immunofluorescence showed that the same enlarged CD5$^+$ MZ area in the chimeric mice as in intact TAN mice (Figure 7e). These results rule out a role for TAN stromal cell in inducing MZ expansion and CD5 expression.

TAN MZ B Cells Show Impaired Functions

MZ B cells are the major responders to T-independent antigens.[9] They constitute the first line of defense against blood-borne Gram-positive bacteria, to which they bind through the bacterial wall polysaccharide residues. We analyzed the ability of TAN MZ B cells to perform this function *in vivo* with TNP-Ficoll, an experimental TI-II type antigen. As expected, Ficoll binding was intense and confined to the marginal zone in B6 spleens (Figure 9a). TAN spleens also showed MZ-restricted Ficoll binding, but contrary to B6, TNP-negative MZ B cells were readily detectable in TAN (Figure 9b). This result could be due, however, to the larger number of MZ B cells in TAN mice. In order to control for cell numbers and TNP-Ficoll concentration, we conducted *in vitro* assays in which total splenocytes were exposed to graded concentrations of TNP-Ficoll. Flow cytometry was then performed to assess TNP binding in each splenic B-cell subset. As expected, TNP binding was only found in MZ B gated cells (data not shown). At low Ficoll concentration ($\leq 5\,\mu$g/ml), TAN and B6 MZ B cells had similar binding ability. B6 showed, however, a dose-dependent increased binding, while TAN MZ B cells showed a binding saturation at higher concentration (Figure 10). Similar results were obtained with either the level of TNP binding as shown in Figure 9, or the percentage of TNP$^+$ MZ B cells (data not shown). Both the *in vivo* and *in vitro* results consequently showed an impaired binding of TI-II antigens by TAN MZ B cells. This difference is not due to a reduced BCR expression, as no difference in IgM expression was found between the two strains.

MZ B cells rapidly migrate into the follicles in response to LPS, where they participate to the immune response by stimulating T cells and differentiating into plasma cells.[33] To assess whether this function was maintained by TAN MZ B cells, we examined the MZ B cells location 3 h after LPS challenge. As expected, B6 MZ B cells migrated inside the follicle (Figure 9c). TAN MZ B cells, however, were still located in the MZ area (Figure 9d), clearly showing an impaired response to LPS. Further staining showed that both CD5$^+$ and CD5$^-$ MZ B cells were retained in the TAN MZ after LPS exposure (Figure 9f). TLR4 complex member MD-1/RP105 was expressed at a lower level by TAN MZ B cells as compared to B6 (Figure 10b and c). We feel, however, that it is unlikely that this small difference is sufficient to account for the failure of TAN MZ B cells to migrate in response to LPS. In addition, CD5$^+$ MZ B cells expressed higher levels of MD-1/RP105 than the CD5$^-$ MZ B cells in both TAN and B6 (Figure 10c), although both CD5$^+$ and CD5$^-$ MZ B cells remained in TAN MZ after LPS exposure (Figure 9f). These results overall suggest that the MD-1/RP105 variations in expression are not responsible for the TAN MZ B cell lack of response to LPS.

Discussion

The TAN strain is phenotypically similar to NZW in several ways with mild production of IgG autoantibody and mild renal pathology.[25,26,34] We have shown that over 70% of the TAN genome was

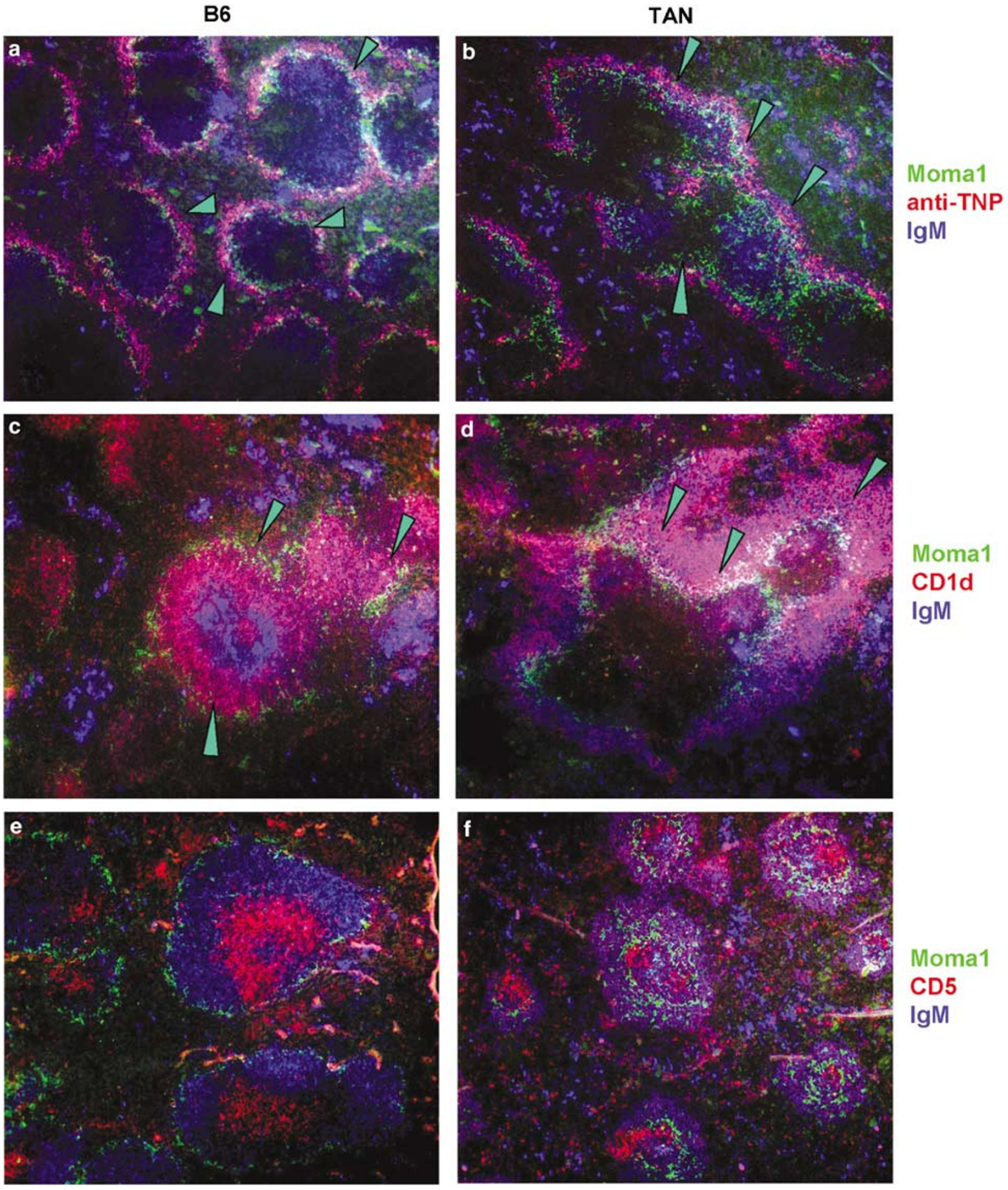

Figure 9 TAN MZ B-cell *in vivo* response to TI antigens. TNP-Ficoll up-take by splenic MZ B cells in B6 (**a**) and TAN (**b**) mice. Mice were killed 30 min after 100 μg TNP-Ficoll intraperitoneal injections. TNP-Ficoll was revealed by anti-TNP (red). B6 spleens showed an intense TNP^+ IgM^+ purple MZ B cell area. TAN MZ also showed TNP-Ficoll binding, but TNP-negative MZ B cells were also present. (**c–f**) MZ B-cells response to LPS in B6 and TAN mice. Mice were killed 3 h after 100 μg LPS intraperitoneal injections. (**c**, **d**) Light purple IgM^+ $CD1d^{hi}$ MZ B cells translocated into follicle demarcated by green Moma-1^+ cells in B6 spleens, but were still in the MZ area in TAN spleens. (**e**, **f**) $CD5^+$ B cells (dark purple) stay in the MZ area after LPS exposure. Representative spleen sections are from three 7-month-old mice per strain. Magnification: $\times$100.

derived from NZW, which would be predictive of these phenotypes. NZM2410, however, was also derived from over 70% of the NZW genome, but showed markedly different clinical outcomes, with a high penetrance of severe proliferative GN that was not observed in TAN. The difference was even

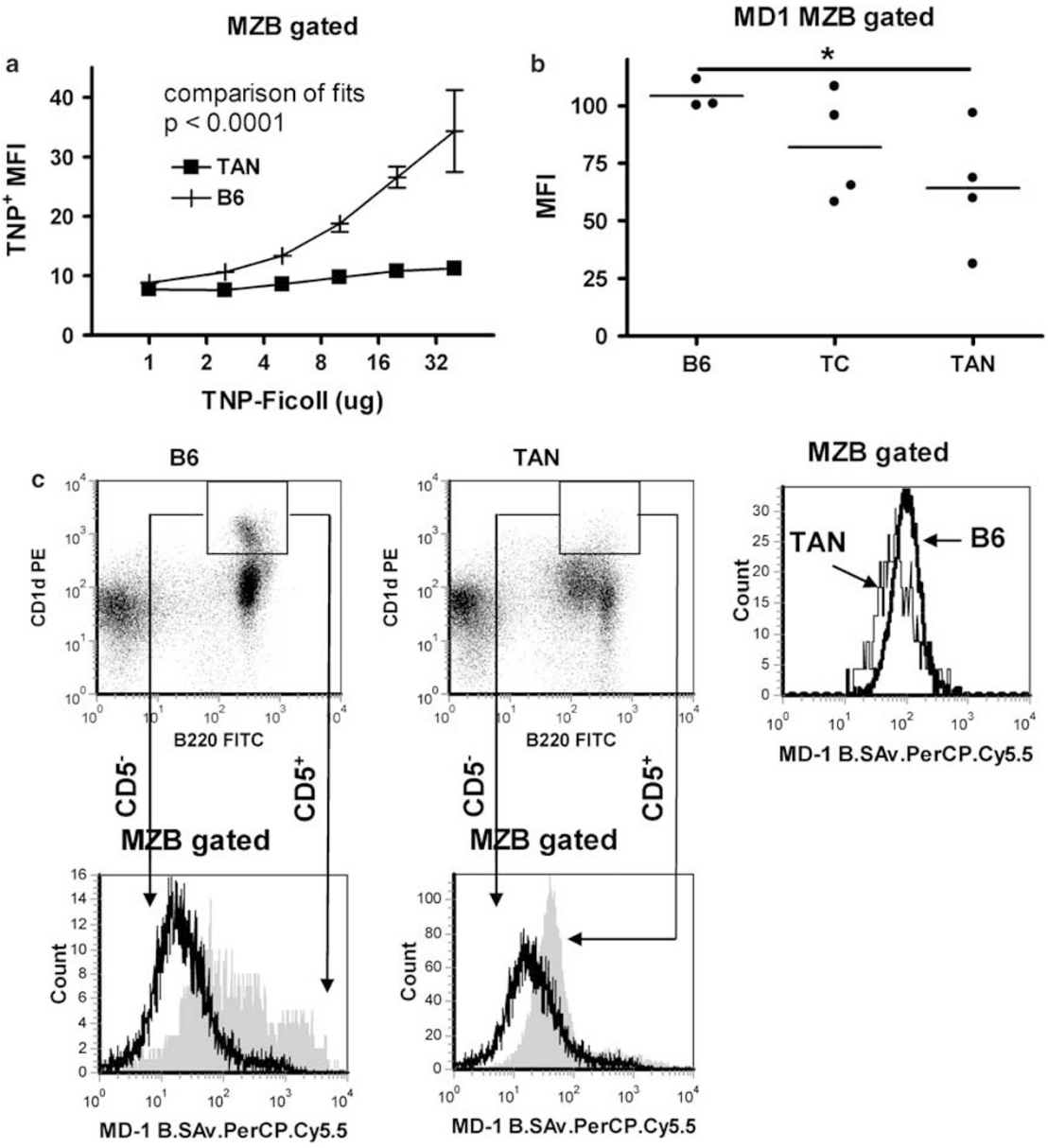

Figure 10 Functional binding of TI-antigens by MZ B cells. (**a**) *In vitro* TNP-Ficoll-binding capability of MZ B cells. Freshly isolated splenocytes were incubated with different concentrations of TNP-Ficoll for 30 min. TNP-Ficoll binding was assayed by flow cytometry with anti-TNP monoclonal antibody on MZ B cells gated with IgM^+ $CD1d^{hi}$. The two curves were statistically significant ($P<0.0001$) as determined by a comparison of fits. (**b**) MD-1/RP105 expression on $B220^+$ $CD1d^{hi}$ MZ B cells. ANOVA test with post-test pair-wise comparisons performed with Bonferoni's corrections ($*P<0.05$). (**c**) Representative FACS plots showing MD-1/RP105 staining on $B220^+$ $CD1d^{hi}$ gated cells MZ B cells. The histogram on the right shows an overlay of B6 and TAN values, with the thin line representing TAN. The histograms at the bottom show overlays based on $CD5^-$ (black line) and $CD5^+$ (grey filled).

more striking with the NZM triple congenic strain B6.TC, which shares with TAN the three *Sle1*, *Sle2* and *Sle3* susceptibility loci that are necessary and sufficient for the development of autoimmune clinical pathology on a B6 background.[6] The results presented here show that expression of these same loci on the TAN genetic background results in a mild autoimmune pathology similar to that of NZW. The absence of *Sle5*, an NZM2410 quantitative trait locus (QTL) linked to anti-dsDNA production,[24] from the TAN genome is unlikely to be critical as other NZM strains also lacking this locus present high levels of severe GN (Waters *et al*[4] and Morel L, unpublished data). TAN and NZM2410 share the same allele at three NZW-derived suppressor loci (*Sles1*, *Sles2*, *Sles4*) but differ at *Sles3*. Interestingly, this locus maps near the *IL2* gene, which is a major susceptibility locus for both type 1 diabetes and experimental autoimmune encephalomyelitis.[35] Whether or not this locus plays a significant role in protecting TAN mice will require an extensive genetic analysis. We have performed a preliminary characterization

of autoimmune disease segregation between the TAN and B6.TC strains by examining the phenotype of their F_1 hybrids. These mice were homozygous for the three *Sle* loci, but heterozygous for the rest of the genome. The F_1 hybrids developed high levels of anti-dsDNA IgG antibodies, but an intermediate penetrance of severe proliferative GN that was not fatal during the first 12 months of life of the animals. These results indicate that the heterozygous TAN genetic background partially suppresses the pathogenic effects of the *Sle1*, *Sle2* and *Sle3* loci, which require an NZM2410 or B6 homozygous background for full expression. Further analysis should delineate the genetic basis for the lupus nephritis resistance offered by the TAN genome.

As lupus susceptibility is a polygenic process that involves multiple molecular and cellular processes, resistance in the TAN model is also likely to be polygenic and multimodal. The present study focuses on B-cell peripheral subsets. Examination of the activation status of $CD4^+$ T cells indicates, however, that the great majority of TAN $CD4^+$ T cells are in a naïve state. Interestingly, the mechanism by which TAN T-cells expressing *Sle* susceptibility loci are kept in check may share a common pathway with B cells as CD5 expression is increased in both lymphocyte populations. CD5 negatively regulates T-cell receptor signaling,[36] and its function in TAN T cells deserves further analysis.

Both the lupus-prone and resistant mice have abnormal splenic B-cell development, as shown by accumulated T1 cells as well as decreased T2 and follicular B cells, suggesting a developmental arrest between the T1 and T2 stages. Immature B cells that just emerged from bone marrow (BM) contain a large number of autoreactive clones, which are largely removed at a negative selection checkpoint during the T1 stage.[37,38] Thus, the accumulation of T1 cells may overload this checkpoint and increase the possibility of autoreactive clones maturating in the periphery. In addition, transitional B cells can present antigens to $CD4^+$ T cells and activate T cells if exogenous costimulation is provided.[39] On the other hand, interactions with activated T cells can also protect immature B cells from negative selection.[39] The accumulation of T1 cells in TAN mice suggests that, similar to NZM2410 and B6.TC, a large number of autoreactive B cells are present in secondary lymphoid organs, and therefore the lupus-resistance occurs downstream of this checkpoint.

Both NZM2410 and B6.TC lupus-prone and TAN lupus-resistant mice have abnormal lymphoid microstructures. This is at least partially due to the fact that they all carry the lupus susceptibility locus *Sle3*, which results in abnormal follicular structures.[40] Our study here shows that the phenotype of the MZ cells correlate to the lupus susceptibility of the mouse strains. Lupus-prone strains NZM and B6.TC lack a marginal zone area, while lupus-resistant TAN mice, on the other hand, have an enlarged marginal zone. This morphological change is not associated, however, with a significant increase in the number of cells with a typical MZ B cell phenotype. MZ B cells have been implicated in lupus autoimmunity[14–16] and early studies have shown that autoreactive B cells could be positively selected into MZ, which could be a mechanism to prevent autoimmunity. In addition, MZ B cells respond more rapidly than follicular B cells to T-dependent antigens and are more potent T-cell activators.[41] Finally, MZ B cells may be exposed to a greater autoantigen load, which can induce T-independent terminal differentiation onto plasma cells.[42] TAN spleens contain large amounts of $CD5^+$ B-1a cells, and a large number of them are located within the marginal zone. As MZ B cells and B-1a cells share a large number of surface markers, it is not possible to determine at this point whether the $CD5^+$ B cells in the TAN MZ are primary MZ B cells that secondarily express CD5, or are primary B-1a cells that have invaded the marginal zone. If the former hypothesis is correct, it would indicate that autoreactivity of MZ B cells is eliminated by the expression of CD5, a negative regulator whose expression has been associated with B-cell anergy.[43] The expression of CD5 thus could increase the activation threshold of TAN MZB cells, which could be responsible for their poor binding of TI-2 antigens and the, failure to respond to LPS. The increased CD9 expression may indicate, however, an increased activation status,[28] although the role of this surface marker in B-cell development is unclear at this point.[44] The latter hypothesis may indicate that the sequestration of autoreactive B-1a cells in the TAN marginal zone has a protective effect on lupus pathogenesis. Functional *in vivo* and *in vitro* experiments are ongoing to address which of these two hypotheses is correct. In any case, the TAN strain presents a functional silencing of a B-cell compartment that combined with other factors, such as low T-cell activity, results in a lupus resistance phenotype.

Taken together, the novel NZM lupus-resistant TAN strain provides a model to elucidate the mechanisms involved in autoimmune pathogenesis. Comparison to the related NZM2410 and B6.TC lupus-prone strains should lead to a better understanding of the genetic determinants of this disease. The characterization of the TAN peripheral B-cell development has already shown a strong correlation between lupus-resistance and the development of an abnormal MZ B-cell population. A better characterization of this population should provide new leads on B-cell tolerance checkpoints.

Acknowledgements

We thank Dr Eric Sobel for helpful suggestions, Daniel Perry, Jessica Lohman and Leilani Zeumer for their excellent work with the mouse colony. This

work was supported by an American Cancer Society (RSG-01-230-01-LIB) and a National Institutes of Health (RO1-AI058150) grants to LM.

References

1 Rudofsky UH, Evans BD, Balaban SL, *et al.* Differences in expression of lupus nephritis in New Zealand mixed H-2z homozygous inbred strains of mice derived from New Zealand black and New Zealand white mice. Origins and initial characterization. Lab Invest 1993;68:419–426.
2 Morel L, Rudofsky UH, Longmate JA, *et al.* Polygenic control of susceptibility to murine systemic lupus erythematosus. Immunity 1994;1:219–229.
3 Morel L, Mohan C, Yu Y, *et al.* Functional dissection of systemic lupus erythematosus using congenic mouse strains. J Immunol 1997;158:6019–6028.
4 Waters ST, Fu SM, Gaskin F, *et al.* NZM2328: a new mouse model of systemic lupus erythematosus with unique genetic susceptibility loci. Clin Immunol 2001;100:372–383.
5 Waters ST, McDuffie M, Bagavant H, *et al.* Breaking tolerance to double stranded DNA, nucleosome, and other nuclear antigens is not required for the pathogenesis of lupus glomerulonephritis. J Exp Med 2004;199:255–264.
6 Morel L, Croker BP, Blenman KR, *et al.* Genetic reconstitution of systemic lupus erythematosus immunopathology with polycongenic murine strains. Proc Natl Acad Sci USA 2000;97:6670–6675.
7 Morel L, Tian X-H, Croker BP, *et al.* Epistatic modifers of autoimmunity in a murine model of lupus nephritis. Immunity 1999;11:131–139.
8 Wakeland EK, Liu K, Graham RR, *et al.* Delineating the genetic basis of systemic lupus erythematosus. Immunity 2001;15:397–408.
9 Martin F, Kearney JF. B-cell subsets and the mature preimmune repertoire. Marginal zone and B1B cells as part of a 'natural immune memory'. Immunol Rev 2000;175:70–79.
10 Berland R, Wortis HH. Origins and functions of B-1 cells with notes on the role of CD5. Ann Rev Immunol 2002;20:253–300.
11 Mohan C, Morel L, Yang P, *et al.* Accumulation of splenic B1a cells with potent antigen-presenting capability in NZM2410 lupus-prone mice. Arthr Rheumat 1998;41:1652–1662.
12 Xu Z, Duan B, Croker BP, *et al.* Genetic dissection of the murine lupus susceptibility locus *Sle2*: contributions to increased peritoneal B-1a cells and lupus nephritis map to different loci. J Immunol 2005;175: 936–943.
13 Wither JE, Roy V, Brennan LA. Activated B cells express increased levels of costimulatory molecules in young autoimmune NZB and (NZB × NZW)F-1 mice. Clin Immunol 2000;94:51–63.
14 Grimaldi CM, Michael DJ, Diamond B. Cutting edge: expansion and activation of a population of autoreactive marginal zone B cells in a model of estrogen-induced lupus. J Immunol 2001;167:1886–1890.
15 Li YJ, Li H, Weigert M. Autoreactive B cells in the marginal zone that express dual receptors. J Exp Med 2002;195:181–188.
16 Wither JE, Loh C, Lajoie G, *et al.* Colocalization of expansion of the splenic marginal zone population with abnormal B cell activation and autoantibody production in B6 mice with an introgressed New Zealand black chromosome 13 interval. J Immunol 2005;175:4309–4319.
17 Sen G, Bikah G, Venkataraman C, *et al.* Negative regulation of antigen receptor-mediated signaling by constitutive association of CD5 with the SHP-1 protein tyrosine phosphatase in B-1B cells. Eur J Immunol 1999;29:3319–3328.
18 Martin F, Kearney JF. Marginal-zone B cells. Nat Rev 2002;2:323–335.
19 Morel L, Yu Y, Blenman KR, *et al.* Production of congenic mouse strains carrying genomic intervals containing SLE-susceptibility genes derived from the SLE-prone NZM2410 strain. Mammal Genome 1996; 7:335–339.
20 Weening JJ, D'Agati VD, Schwartz MM, *et al.* The classification of glomerulonephritis in systemic lupus erythematosus revisited. J Am Soc Nephrol 2004;15: 241–250.
21 Xu Z, Duan B, Croker BP, *et al.* STAT4 deficiency reduces autoantibody production and glomerulonephritis in a mouse model of lupus. Clin Immunol 2006;120:189–198.
22 Boackle SA, Holers VM, Chen XJ, *et al.* Cr2, a candidate gene in the murine Sle1c lupus susceptibility locus, encodes a dysfunctional protein. Immunity 2001;15:775–785.
23 Sobel ES, Mohan C, Morel L, *et al.* Adoptive transfer of NZM-derived lupus susceptibility locus SLE1 on murine chromosome 1 by bone marrow. Arthr Rheumat 1997;40:1072.
24 Morel L, Mohan C, Yu Y, *et al.* Multiplex inheritance of component phenotypes in a murine model of lupus. Mammal Genome 1999;10:176–181.
25 Braverman IM. Study of autoimmune disease in New Zealand mice. I. genetic features and natural history of NZB, NZY and NZW strains and NZB-NZW hybrids. J Invest Dermatol 1968;50:483–499.
26 Kelley VE, Winkelstein A. Age- and sex-related glomerulonephritis in New Zealand white mice. Clin Immunol Immunopathol 1980;16:142–150.
27 Chen Y, Cuda C, Morel L. Genetic determination of T cell help in loss of tolerance to nuclear antigens. J Immunol 2005;174:7692–7702.
28 Won WJ, Kearney JF. CD9 is a unique marker for marginal zone B cells, B1 cells, and plasma cells in mice. J Immunol 2002;168:5605–5611.
29 Cyster JG. Chemokines, sphingosine-1-phosphate, and cell migration in secondary lymphoid organs. Ann Rev Immunol 2005;23:127–159.
30 Karlsson MCI, Guinamard R, Bolland S, *et al.* Macrophages control the retention and trafficking of B lymphocytes in the splenic marginal zone. J Exp Med 2003;198:333–340.
31 Nolte MA, Arens R, Kraus M, *et al.* B cells are crucial for both development and maintenance of the splenic marginal zone. J Immunol 2004;172:3620–3627.
32 Srivastava B, Quinn III WJ, Hazard K, *et al.* Characterization of marginal zone B cell precursors. J Exp Med 2005;202:1225–1234.
33 Groeneveld PHP, Erich T, Kraal G. *In vivo* effects of LPS on lymphocyte-B subpopulations—migration of marginal zone-lymphocytes and IgD-blast formation in the mouse spleen. Immunobiol 1985;170:402–411.

34 Fernandes G, Yunis EJ, Good RA. Age and genetic influence on immunity in NZB and autoimmune-resistant mice. Clin Immunol Immunopathol 1976;6: 318–333.
35 Encinas JA, Wicker LS, Peterson LB, *et al.* QTL influencing autoimmune diabetes and encephalomyelitis map to a 0.15-cM region containing *Il2*. Nat Genet 1999;21:158–160.
36 Tarakhovsky A, Kanner SB, Hombach J, *et al.* A role for Cd5 in TCR-mediated signal-transduction and thymocyte selection. Science 1995;269:535–537.
37 Wardemann H, Yurasov S, Schaefer A, *et al.* Predominant autoantibody production by early human B cell precursors. Science 2003;301:1374–1377.
38 Srivastava B, Lindsley RC, Nikbakht N, *et al.* Models for peripheral B cell development and homeostasis. Semin Immunol 2005;17:175–182.
39 Chung JB, Wells AD, Adler S, *et al.* Incomplete activation of CD4T cells by antigen-presenting transitional immature B cells: implications for peripheral B and T cell responsiveness. J Immunol 2003;171:1758–1767.
40 Mohan C, Yu Y, Morel L, *et al.* Genetic dissection of Sle pathogenesis: Sle3 on murine chromosome 7 impacts T cell activation, differentiation, and cell death. J Immunol 1999;162:6492–6502.
41 Attanavanich K, Kearney JF. Marginal zone, but not follicular B cells, are potent activators of naive CD4T cells. J Immunol 2004;172:803–811.
42 Mandik-Nayak L, Racz J, Sleckman BP, *et al.* Autoreactive marginal zone B cells are spontaneously activated but lymph node B cells require T cell help. J Exp Med 2006;203:1985–1998.
43 Hippen KL, Tze LE, Behrens TW. CD5 maintains tolerance in anergic B cells. J Exp Med 2000;191:883–889.
44 Cariappa A, Shoham T, Liu HY, *et al.* The CD9 tetraspanin is not required for the development of peripheral B cells or for humoral immunity. J Immunol 2005;175:2925–2930.